

Mechanical behaviour of beech glued laminated timber columns subjected to compression loading

Monika Zeilhofer
Technical University Munich, Chair of Wood Science, Professorship of Wood Technology
Munich, Germany



Mechanical behaviour of beech glued laminated timber columns subjected to compression loading

1. Introduction and relevance of the topic

The high compression strength of beech glued laminated timber may allow an efficient application of this hardwood species in building components stressed in compression, like columns or compression members in a truss system. Compression loading causes either stress or stability failure. Exceeding the material strength provokes stress failure while disproportionate horizontal deformations in combination with a high decrease of load carrying capacity lead to stability failure.

The design code DIN EN 1995-1-1:2010 [1] offers two approaches to determine the load carrying capacity of slender timber members under compression loading, namely the equivalent member method and a second order theory analysis. The equivalent member method was derived from a strain-based modelling on spruce glued laminated timber columns and considers stability issues by a reduction of the material strength. An increase of the load due to horizontal deformations of the column is accounted for in the second order theory analysis. Theiler [2] found a good accordance between calculated load carrying capacities by means of the equivalent member method with experimentally tested as well as simulated spruce glued laminated timber columns under compression loading. He suggested improvements in the design of spruce glued laminated timber columns under compression loading with second order theory analysis regarding the stiffness and imperfection parameters [2]. For high quality beech glued laminated timber under compression loading, the DIN EN 1995-1-1:2010 [1] equivalent member method design seems to overestimate the load carrying capacity of simulated and experimentally tested columns according to Ehrhart et al. [3] due to a different strength to stiffness ratio for hardwoods than for softwoods. In the work of Ehrhart et al. [3] big cross sections were tested experimentally, which is not representative for applications in truss systems. This indicates the necessity to examine the DIN EN 1995-1-1:2010 [1] calculation methods for beech glued laminated timber columns employing material from low to high quality with small cross sections.

In this study compression tests on beech glued laminated timber columns of different slenderness ratios with small cross sections were performed. The measured load carrying capacities are compared with calculation approaches given in DIN EN 1995-1-1:2010 [1]. A strain-based modelling is implemented and verified by the testing outcomes. This work summarizes the Master's Thesis 'Mechanical behaviour of beech glued laminated timber columns subjected to compression loading' [4] written at Technical University Munich, Chair of Wood Science, Professorship of Wood Technology under the supervision of Maximilian Westermayr and Jan-Willem van de Kuilen within the frame of the research project "Beech Connect".

2. Materials and methods

2.1. Material

The origin of the raw beech lamellas was Central Germany. Half of the lamellas were provided from the sawmill *Pollmeier* with the trade name *Common Shop*, consisting of timber of the lowest sorting class specifically defined by the producer with visual grading. It contained a high number of growth defects, like knots, fibre deviation, cracks, discolouration and pith. This sorting process did not correspond with the strength grading criteria in DIN

EN 408:2012 [5]. The other half of the boards were available at TU Munich, Chair of Wood Science, including wood with middle or high quality that was free of remarkable fibre deviation and had a low number of wood defects.

The moisture content, the density and the dynamic Modulus of Elasticity (MoE) were measured on the original board length of approximately 3100 mm for all lamellas. The raw lamellas had a mean moisture content of 10 % with a COV of 12 %, a mean density of 720 kg/m³ with a COV of 5 % and a mean dynamic MoE of 13300 N/mm² with a COV of 17 %. The dynamic MoE, with values between 8500 N/mm² and 19000 N/mm², represents a natural spread of properties for beech wood of low to high quality.

No visual grading of the raw lamellas according to DIN EN 408:2012 [5] was performed in order to cover the full range of wood qualities. The lamellas were only sorted by their dynamic MoE to estimate the quality of the material. Similar to the work of Westermayr et al. [6], two glulam specimen setups were generated. In the homogeneous setup, all four lamellas within one specimen had a similar dynamic MoE including low as well as high values (Figure 1). In the combined setup, the dynamic MoE of the two outer lamellas outraged the dynamic MoE of the two inner lamellas with increasing ratios between the dynamic MoE of the outer lamellas and the dynamic MoE of the inner lamellas (Figure 2). With the applied sorting process of the lamellas, the predictability of the load carrying capacities of the specimens by the dynamic MoE should be assessed. The lamellas, sorted by their dynamic MoEs and planed to a thickness of 20 mm, were bonded to one glued laminated timber member with the MUF adhesive system *Kauramin 683+688* from *BASF* by *Schaffitzel Holzindustrie*.

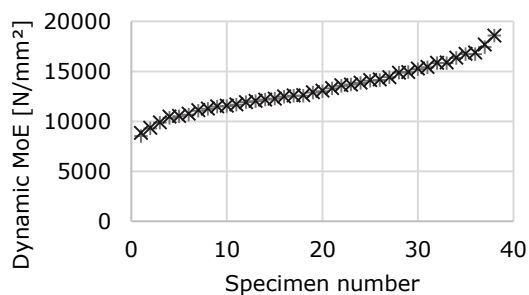


Figure 1: Homogeneous specimens - Dynamic MoEs of the inner and outer lamellas

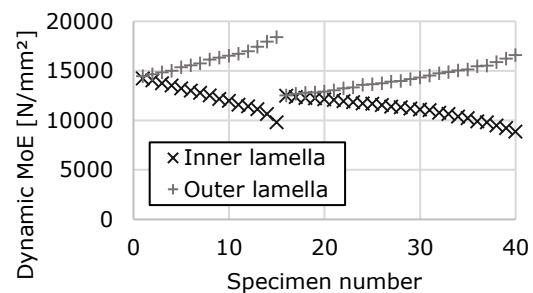


Figure 2: Combined specimens - Dynamic MoEs of the inner and outer lamellas

The dynamic MoE of the entire specimen was determined on the final length of the specimens. The homogeneous setup results in a high scatter of dynamic MoEs of the entire specimens. On the contrary, the dynamic MoEs of the entire combined specimens exhibit a low scatter similar to the findings in Westermayr et al. [6]. For the homogeneous specimens, the mean dynamic MoEs of the raw lamellas within one specimen achieve a correlation $R^2 = 0.96$ with the dynamic MoEs of the entire specimen as already illustrated in Westermayr et al. [6].

In total, 57 specimens were available for testing with two different slenderness ratios. The specimens had a length of 1040 mm ($\lambda = 45$) as well as 1850 mm ($\lambda = 80$) and a cross section of 80 x 80 mm². 19 specimens of slenderness ratio $\lambda = 45$ were tested for buckling around the y-axis, which defines a horizontal movement of the specimen perpendicular to the adhesive layer. 18 specimens with $\lambda = 45$ were subjected to buckling around the z-axis, which corresponds with a horizontal movement of the specimen parallel to the adhesive layer. Both directions were assessed to investigate an influence of the orientation of the adhesive layer to the buckling direction on the load carrying capacity of the specimens. The specimens with slenderness ratio $\lambda = 80$ were all assessed for buckling around the y-axis. In every slenderness ratio/buckling direction subset, the amounts of homogeneous and combined specimens were approximately equal (Table 1).

Table 1: Number (n) of specimens for the different slenderness ratios and buckling directions as well as distinction into homogeneous and combined specimens.

Slenderness	Length [mm]	Buckling direction	n _{total}	n _{homogeneous}	n _{combined}
45	1040	y	19	10	9
45	1040	z	18	8	10
80	1850	y	20	10	10
<i>TOTAL</i>			57	28	29

2.2. Methods

Destructive and non-destructive measurements

Before performing the destructive compression tests, the dynamic MoE, the density and the moisture content of the raw lamellas as well as of the entire specimens were determined. The dynamic MoE was calculated by means of Eigenfrequency and adjusted to 12 % moisture content according to Unterwieser & Schickhofer [7]. The initial deformation was measured as the deviation of the beech glued laminated timber column from an ideal straight line.

During the experimental testing, the beech glued laminated timber columns were mounted on bearings flexible in solely one direction. The load was applied with a hydraulic testing machine depicted in Figure 3.

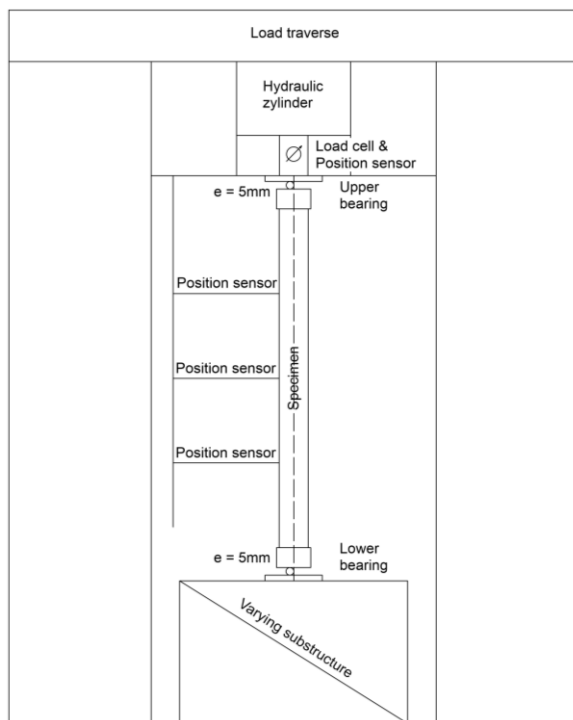


Figure 3: Sketch of the testing machine.

The experiments were performed path-controlled until a decrease in the load was visible. One experiment took between five and fifteen minutes. An eccentricity $e = 5\text{ mm}$ was applied to control the buckling direction of the specimens and prohibit damage to the measurement equipment. The horizontal displacements in buckling direction were assessed in the middle and both quarter points of the specimens.

Strain-based modelling

The equivalent member method in DIN EN 1995-1-1:2010 [1] was derived from a strain-based modelling on spruce glued laminated timber columns with stochastically simulated material properties [8]. A material model was used, which was specifically developed for spruce glued laminated timber [9]. It considers linear elastic material behaviour under tensile loading and a non-linear plastic material behaviour under compression loading. The load carrying capacity was investigated for different slenderness ratios and the factor k_c was defined (Equation 10). In contrast to spruce wood, beech glued laminated timber from similar cross section, origin and setup, regarding the dynamic MoE like the tested material in this work, gains a higher strength to stiffness ratio [6]. A strain-based modelling with a material model for beech glued laminated timber is introduced to review the DIN EN 1995-1-1:2010 [1] buckling curve.

Glos et al. [10] developed a material model for high-strength beech glued laminated timber from the material model for spruce glued laminated timber [9]. Equation 1 [10] describes the material behaviour under compression loading.

$$\sigma_c = \frac{\epsilon + k_1 * \epsilon^4}{k_2 + k_3 * \epsilon + k_4 * \epsilon^4} \quad 1$$

The stress σ_c results from the strain ϵ across the cross section and the parameters k_i (equations 2 - 5), which depend on the MoE for compression $E_{c,0}$, the compression strength $f_{c,0}$, the remaining compression strength after reaching maximum compression strength $f_{c,u,0}$ and the strain at maximum compression strength $\epsilon_{c,0}$.

$$k_1 = \frac{f_{c,u,0}}{3 * E_{c,0} * \epsilon_c^4 * (1 - \frac{f_{c,u,0}}{f_{c,0}})} \quad 2 \quad k_3 = \frac{1}{f_{c,0}} - \frac{4}{3} * \frac{1}{E_{c,0} * \epsilon_{c,0}} \quad 3$$

$$k_2 = \frac{1}{E_{c,0}} \quad 4 \quad k_4 = \frac{1}{3 * E_{c,0} * \epsilon_c^4 * (1 - \frac{f_{c,u,0}}{f_{c,0}})} \quad 5$$

Ehrhart et al. [3] and Theiler [2] employed equation 6 to calculate the remaining compression strength $f_{c,u,0}$, which was determined for spruce glued laminated timber [11].

$$f_{c,u,0} = 0.85 * f_{c,0} \quad 6$$

Equation 6 is also applied in this work for beech glued laminated timber as no own experimental data was available to determine the remaining compression strength $f_{c,u,0}$. The limit for the strain at maximum compression strength $\epsilon_{c,0}$ is given by equation 7 [10].

$$\epsilon_{c,0} \geq \frac{4}{3} * \frac{f_{c,0}}{E_{c,0}} \quad 7$$

O'Halloran [12] found, by means of experimental investigations, equation 8 for the strain at maximum compression strength $\epsilon_{c,0}$. Equation 8 was approved by Glos [11] and Frese et al. [13] for spruce glued laminated timber.

$$\epsilon_{c,0} = 1.25 * \frac{f_{c,0}}{E_{c,0}} \quad 8$$

Equation 8 does not fulfil the criterion 7 [10]. Ehrhart et al. [3], however, used equation 8. In this work, equation 9 was developed representing the closest solution to both the criterion 7 and equation 8.

$$\epsilon_{c,0} = 1.34 * \frac{f_{c,0}}{E_{c,0}} \quad 9$$

The strain-based modelling is performed according to Glos [9] with a fixed assumed shape of the buckling curve. A Visual Basic Script Application with Microsoft Excel 2016 is implemented to execute the strain-based modelling.

3. Results and Discussion

3.1. Experimental investigation

Influence of specimen setup on the load carrying capacity

The buckling strength $f_{crit,0}$ is defined as the load carrying capacity of the specimen divided by the specimen cross section. The buckling strength $f_{crit,0}$ decreases with increasing specimen length while the COV increases as visible in Table 2. The growth in scatter may arise from a wider range of properties with higher specimen length.

The mean buckling strengths $f_{crit,0}$ for homogeneous (H) and combined (C) specimens do not differ significantly. The minimum and maximum buckling strength $f_{crit,0}$ of the homogeneous specimens are lower and higher respectively than the minimum and maximum buckling strength $f_{crit,0}$ of the combined specimens. This indicates that a combination of lamellas with low and high dynamic MoEs offers the possibility to reduce the spread in buckling strengths $f_{crit,0}$ in comparison to a homogeneous specimen setup. A quantification of the effect of different ratios of dynamic MoEs between outer and inner lamellas on the buckling strength $f_{crit,0}$ was not possible.

Table 2: Mean buckling strength $f_{crit,0}$ of the specimens for different slenderness ratios, specimen setups and buckling directions.

Slenderness	Setup	n	Mean $f_{crit,0}$ [N/mm ²]	Min $f_{crit,0}$ [N/mm ²]	Max $f_{crit,0}$ [N/mm ²]	COV F
45y	H	10	46	31	53	0.14
	C	9	41	36	48	0.11
45z	H	8	38	27	48	0.16
	C	10	41	37	48	0.08
80y	H	10	28	17	43	0.26
	C	10	30	23	38	0.16

Taking particularly the homogeneous specimens into account, a correlation between the mean dynamic MoE of the lamellas within one specimen and the buckling strength $f_{crit,0}$ of $R^2 = 0.51$ and a $R^2 = 0.74$ can be found for specimens of slenderness ratio $\lambda = 45$ and $\lambda = 80$, respectively. Similar correlations can be achieved between the dynamic MoE of the entire specimens and the buckling strengths $f_{crit,0}$. The correlation between dynamic MoE and buckling strength $f_{crit,0}$ may be traced back to the correlation between dynamic and static MoE for beech glued laminated timber [6]. The improvement of the correlation between dynamic MoE and buckling strength $f_{crit,0}$ with increasing specimen length may be explained with the measurement of the dynamic MoE on the original board length of 3100 mm. The properties of a specimen with 1850 mm may be represented more appropriately by the dynamic MoE measured on the original board length than of the shorter specimens with a length of 1050 mm. The increasing correlation between the dynamic MoE and the buckling strength $f_{crit,0}$ with increasing slenderness ratio may also result from the increasing effect of the stiffness on the buckling behaviour for higher slenderness ratios.

The buckling strengths $f_{crit,0}$ of specimens buckling around the y- and the z-axis are not significantly different as visible in Table 2. The specimens buckling around the z-axis exhibit a slightly lower scatter in their buckling strengths $f_{crit,0}$ than the specimens buckling around the y-axis probably deriving from a lower scatter in dynamic MoE.

Test results in comparison to DIN EN 1995-1-1:2010 [1] design methods

DIN EN 1995-1-1:2010 [1] describes the relationship between slenderness and load carrying capacity in the buckling curve. The equivalent member method and the second order theory analysis require strength and stiffness values to calculate the load carrying capacity. Table 3 provides an overview of the applied strength and stiffness features from

Westermayr et al. [6], investigated for beech glued laminated timber of the same cross section, origin and similar specimen setup regarding the dynamic MoE, like the specimens in this work.

Table 3: Applied strength and stiffness properties [6].

Characteristic compression strength $f_{c,0,k}$ [N/mm ²]	53
Characteristic bending strength $f_{m,k}$ [N/mm ²]	53
Characteristic tensile strength $f_{t,0,k}$ [N/mm ²]	39
Characteristic compression stiffness $E_{c,0,05}$ [N/mm ²]	11000
Mean compression stiffness $E_{c,mean}$ [N/mm ²]	13670
Characteristic tensile stiffness $E_{t,0,k}$ [N/mm ²]	10870

To estimate the buckling strength $f_{crit,0}$, intended and unintended eccentricities of the applied load must be assessed besides the strength and stiffness properties. The intended eccentricity of load application during the experiments was $e = 5$ mm. The unintended eccentricities consist solely of an initial deformation of the specimens, as geometrical imperfections, such as a tilting of the specimen or an unintended eccentricity of loading, can be excluded due to the testing setup. Structural imperfections, resulting from an asymmetrical distribution of strength and stiffness properties across the cross section, can be neglected due to the symmetrical specimen setup. Section 10 of DIN EN 1995-1-1:2010 [1] limits the eccentricity considered in the design of slender compression members to $l/500$, which seems to apply to the equivalent member method calculation. In the second order theory analysis, structural and geometrical imperfections are accounted for with $w_0 = l/400$. Considering additional bending stresses caused by the eccentricity $e = 5$ mm, the calculated buckling strengths $f_{crit,0}$ by DIN EN 1995-1-1:2010 [1] methods employing strength and stiffness properties from Westermayr et al. [6] (Table 3) are discussed with the measured buckling strengths $f_{crit,0}$ in Figure 4.

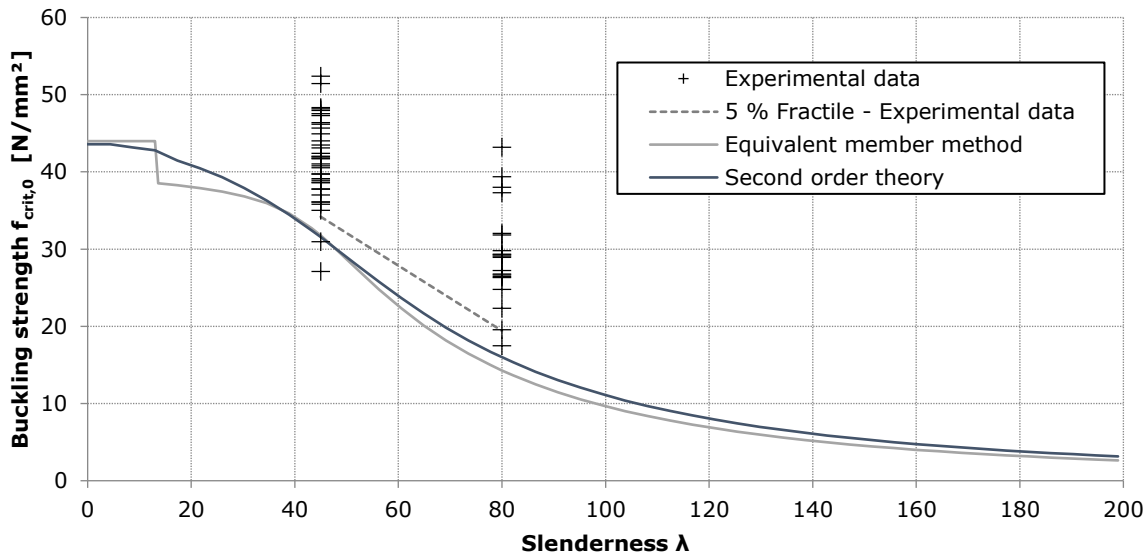


Figure 4: Measured buckling strengths $f_{crit,0}$ (crosses) and 5% fractiles (dotted line) in comparison to calculated buckling strengths $f_{crit,0}$ by DIN EN 1995-1-1:2010 [1] (solid lines) with strength and stiffness properties from Westermayr et al. [6] (Table 3) and eccentricity $e = 5$ mm.

The buckling curves according to DIN EN 1995-1-1:2010 [1] equivalent member method and second order theory analysis exhibit only small differences. The unsteadiness in the equivalent member method curve at a slenderness ratio λ of approximately 13 derives from a change of quadratic to a linear relationship between compression loading and compression strength.

The measured buckling strengths $f_{crit,0}$ are underestimated with DIN EN 1995-1-1:2010 [1] calculation methods. The underestimation of the measured buckling strengths $f_{crit,0}$ by DIN EN 1995-1-1:2010 [1] is more pronounced for slenderness ratio $\lambda = 80$ than $\lambda = 45$. For slenderness ratio $\lambda = 45$, equivalent member method and second order theory analysis yield similar results, while for slenderness ratio $\lambda = 80$, the second order theory analysis determines buckling strengths $f_{crit,0}$ closer to the experimental data.

A reason for the underestimation of the measured buckling strengths $f_{crit,0}$ by DIN EN 1995-1-1:2010 [1] design can be found in the consideration of the applied eccentricity $e = 5$ mm and the initial deformation of the specimens. The initial deformation of the specimens - $w_{0,measured,mean} = l/2500$, $w_{0,measured,0.95} = l/770$, $w_{0,measured,max} = l/625$ - are smaller than the imperfections suggested by DIN EN 1995-1-1:2010 [1], probably due to the storage in normal climate after planing. In a realistic situation, the initial deformations may reach higher values due to the influence of moisture changes during transportation and storage at a construction site, as well as a tilted installation. In similar experiments, Ehrhart et al. (2019) who applies eccentricities of $l/380$ and $l/570$ neglects the eccentricity in the calculation. The eccentricity of $e = 5$ mm in this work equals values of $l/208$ and $l/360$. A comparison of the calculated buckling strengths $f_{crit,0}$ with eccentricities of $e = 5$ mm and $e = 0$ mm with the measured buckling strengths $f_{crit,0}$ is shown in Figure 5.

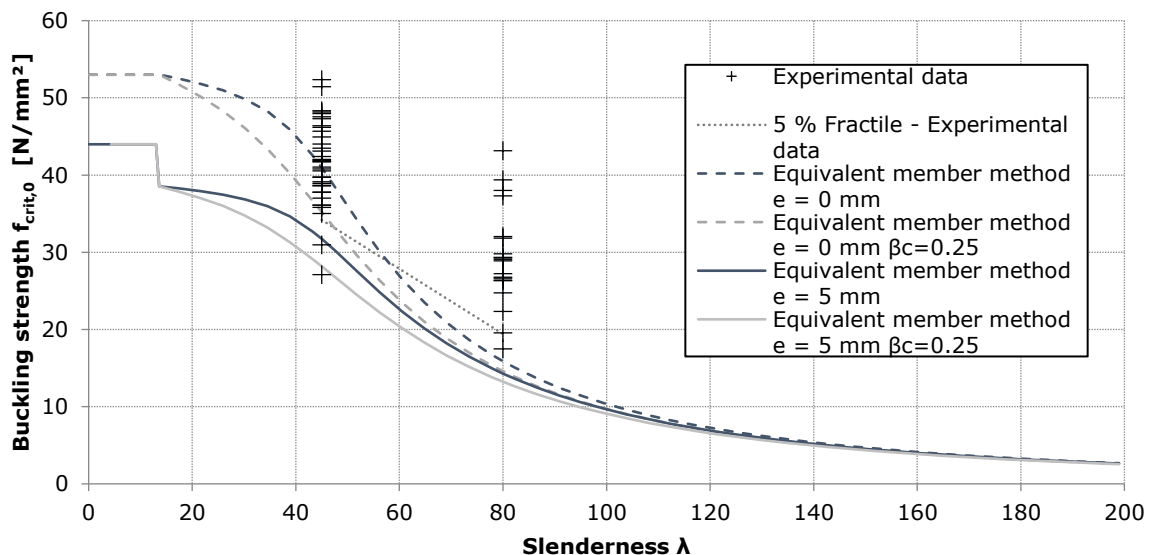


Figure 5: Measured buckling strengths in comparison to calculated buckling strengths $f_{crit,0}$ with equivalent member method according to DIN EN 1995-1-1:2010 [1]. Eccentricities of $e = 5$ mm (solid lines) and $e = 0$ mm (dashed lines), imperfection parameter $\beta_c = 0.1$ and $\beta_c = 0.25$.

Calculating the buckling strengths $f_{crit,0}$ by neglecting the eccentricity leads to an overestimation of the measured buckling strengths $f_{crit,0}$ for slenderness ratio $\lambda = 45$. On the contrary, hardly any change in the calculated buckling strengths $f_{crit,0}$ by neglecting the eccentricity is visible for slenderness ratio $\lambda = 80$. A reasonable compromise between an eccentricity of $e = 5$ mm and $e = 0$ mm may be found by considering an eccentricity of $e = 5$ mm - $(l/500 - l/770)$ in the calculation. This equals the eccentricity $e = 5$ mm minus the difference between the initial deformation considered in the equivalent member method calculation reduced by the 95 % fractile of the measured initial deformations. The 5 % fractiles of the measured buckling strengths $f_{crit,0}$ show a high accordance with these calculated buckling strengths $f_{crit,0}$ with the reduced eccentricity of $e = 5$ mm - $(l/500 - l/770)$ for slenderness ratio $\lambda = 45$.

The small initial deformations of the columns may also be a reason for the underestimation of the measured buckling strengths $f_{crit,0}$ by the second order theory analysis. The modification of the initial deformation in the design code from $w_0 = l/400$ to the measured 95 % fractile of the initial deformation of the specimens of $w_0 = l/770$ contributes to a better accordance between the measured and calculated buckling strengths $f_{crit,0}$ for specimens of slenderness ratio $\lambda = 45$. A slight overestimation of the measured buckling strengths

$f_{crit,0}$ occurs using the mean initial deformation for slenderness ratio $\lambda = 45$. For slenderness ratio $\lambda = 80$, the calculated buckling strength $f_{crit,0}$ is hardly changed by employing different initial deformations.

The DIN EN 1995-1-1:2010 [1] buckling curves have a higher gradient than the slope of the 5 % fractiles of the measured buckling strengths $f_{crit,0}$. The equivalent member method was derived from a strain-based modelling on spruce glued laminated timber [8]. Spruce glued laminated timber shows a strength to stiffness ratio of 1/420 to 1/370 while beech glued laminated timber in this project [6], exhibits a strength to stiffness ratio of 1/208. Ehrhart et al. [14] found a strength to stiffness ratio of approximately 1/250 for high-quality beech glued laminated timber. An increase of the strength to stiffness ratio results in a decrease of the slope of the buckling curve [15]. The factor k_c (Equation 10) defines the shape of the buckling curve and depends on strength and stiffness properties, as well as geometry features of the specimens, but also on the critical relative slenderness $\lambda_{rel,0}$ and the imperfection parameter β_c .

$$k_c = \frac{1}{k + \sqrt{k^2 - \lambda_{rel}^2}} \quad 10$$

$$\lambda_{rel} = \frac{\lambda}{\pi} \sqrt{\frac{f_{c,0,k}}{E_{0,05}}} \quad 11$$

$$k = 0,5 * [1 + \beta_c * (\lambda_{rel} - \lambda_{rel,0}) + \lambda_{rel}^2] \quad 12$$

A decrease of the slope of the buckling curve can be realised in the equivalent member method by an enlargement of the imperfection parameter β_c . Applying the imperfection parameter $\beta_c = 0.25$ leads to a good accordance between the slope of the calculated and measured 5 % fractile buckling strengths $f_{crit,0}$ as visible in Figure 5. The change of β_c affects the buckling strength $f_{crit,0}$ of specimens with slenderness ratio $\lambda = 45$ much more than the buckling strengths $f_{crit,0}$ of specimens with slenderness ratio $\lambda = 80$.

3.2. Comparison of the modelling results with experimental data and DIN EN 1995-1-1:2010 [1]

Blaß [16] and Theiler [2] proved that strain-based modelling can reproduce buckling experiments on spruce glued laminated timber appropriately. Ehrhart et al. [3] confirmed those findings for beech glued laminated timber columns.

In Figure 6, the buckling strengths $f_{crit,0}$ for different slenderness ratios, obtained from strain-based modelling are compared with the experimental data as well as the calculated buckling strengths $f_{crit,0}$ according to DIN EN 1995-1-1:2010 [1] equivalent member method with $\beta_c = 0.1$ and $\beta_c = 0.25$. An eccentricity of $e = 5$ mm is considered in the calculated buckling strengths $f_{crit,0}$. Strength and stiffness values from Table 2 [6] are employed.

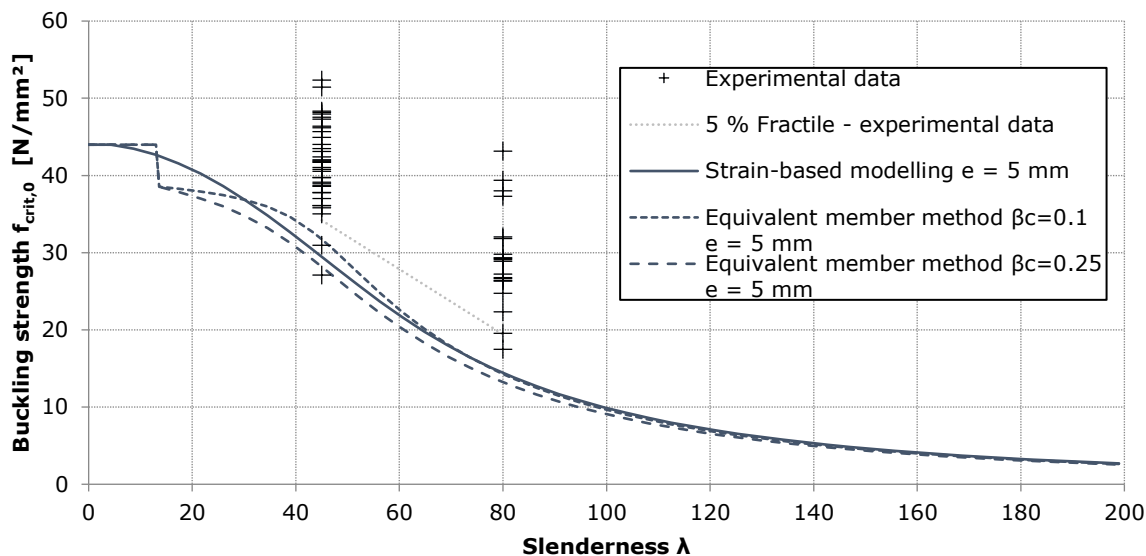


Figure 6: Comparison of the measured and calculated buckling strengths $f_{crit,0}$ by DIN EN 1995-1-1:2010 [1] equivalent member method with $\beta_c = 0.1$ (small dashed lines) and $\beta_c = 0.25$ (big dashed lines) as well as strain-based modelling (solid lines) with an eccentricity of $e = 5$ mm.

The strain-based modelling underestimates the buckling strengths $f_{crit,0}$ of the specimens. The strain-based modelling buckling curve matches more appropriate with the equivalent member method curve with $\beta_c = 0.25$ than with $\beta_c = 0.1$ for an eccentricity $e = 5$ mm. All calculated buckling curves yield higher slopes than the 5 % fractiles of the measured buckling strengths $f_{crit,0}$ where the DIN EN 1995-1-1:2010 [1] equivalent member method with $\beta_c = 0.25$ shows the closest gradient followed by the strain-based modelling.

4. Summary and conclusions

The load carrying capacities measured on beech glued laminated timber lay on the safe side of the calculated load carrying capacities by means of DIN EN 1995-1-1:2010 [1]. Due to the different strength to stiffness ratio of beech wood compared to spruce wood, an adjustment of the imperfection parameter β_c in DIN EN 1995-1-1:2010 [1] equivalent member may lead to a better accordance between calculated and measured buckling curve. The suggested revisions in the equivalent member method can be verified by a strain-based modelling applying a material model for beech glued laminated timber [10]. The tested material shows small geometrical imperfections. In practical cases, larger eccentricities or imperfections can affect the load carrying capacity.

The dynamic MoEs of glued laminated timber members with similar dynamic MoEs of the lamellas exhibit a good correlation with their measured load carrying capacity. A combination of outer lamellas with higher dynamic MoEs than the inner lamellas leads to a reduction in the scatter of load carrying capacities of the specimens.

5. Outlook

More tests on columns with different slenderness ratios should be performed to encourage the suggested adjustment of the imperfection parameter β_c in DIN EN 1995-1-1:2010 [1] equivalent member method. The scientific lamella arrangement within the glued laminated timber members by means of the dynamic MoE in this study should be complemented with an industrial lamella arrangement where the single lamellas are chosen from strength classes with scattering dynamic MoE. Additional buckling tests could be performed where the raw lamellas are graded and sorted into strength classes in order to achieve a testing setup representative for practical cases.

In practical cases, members of a truss system and columns are subjected to long term loading, creep and moisture changes. An increase of the moisture content of beech glued laminated timber columns yields a significant decrease in strength and stiffness properties

([17] and [16]). Thus, the effects of moisture changes, creep behaviour and long-term loading on the load carrying capacity of beech glued laminated timber columns need to be examined by further research.

6. References

- [1] DIN EN 1995-1-1, Design of timber structures – Part 1-1: General – Common Rules, 2010.
- [2] M. Theiler, "Stabilität von axial auf Druck beanspruchten Bauteilen aus Vollholz und Brettschichtholz. In German. Dissertation. ETH Zürich," 2014.
- [3] T. Ehrhart, R. Steiger, P. Palma, E. Gehri and A. Frangi, "Compressive strength and buckling resistance of GLT columns made of European beech (*Fagus sylvatica*)," *INTER Conference 52, Tacoma, USA, Paper 52-12-1*, 2019.
- [4] M. Zeilhofer, Mechanical behaviour of beech glued laminated timber columns subjected to compression loading. Master's Thesis. Technical University Munich, München, 2019.
- [5] DIN EN 408:2012, Strength grading of wood - Part 5: Sawn hard wood, 2012.
- [6] M. Westermayr, P. Stapel and J.-W. van de Kuilen, "Tensile and Compression Strength of Small Cross Section Beech Glulam Members," *INTER Conference 51, Tallinn, Estonia, Paper No. 51-12-2*, 2018.
- [7] H. Unterwieser and G. Schickenhofer, "Influence of moisture content of wood on sound velocity and dynamic MoE of natural frequency- and ultrasonic runtime measurement," *European Journal of Wood and Wood Products*. (69), pp. 171-181, 2011.
- [8] H. Blaß, "Design of columns," *Proceeding of the 1991 International Timber Engineering Conference, London, United Kingdom*, 1991.
- [9] P. Glos, "Zur Bestimmung des Festigkeitsverhalten von Brettschichtholz bei Druckbeanspruchung aus Werkstoff- und Einwirkungskenngrößen. In German. Dissertation," *Laboratorium für den konstruktiven Ingenieurbau (LKI) Technische Universität München*, 1978.
- [10] P. Glos, J. Denzler and P. Linsemann, "Strength and stiffness behaviour of beech laminations for high strength glulam," *CIB-W18 Proceedings 37, Paper No. 37-6-3, Edingburgh, Ireland*, 2004.
- [11] P. Glos, "Zur Modellierung des Festigkeitsverhaltens von Bauholz bei Druck-, Zug- und Biegebeanspruchung. In German," *Laboratorium für den konstruktiven Ingenieurbau (LKI) Technische Universität München*, 1981.
- [12] M. O'Halloran, Curvilinear stress-strain relationship for wood in compression. Dissertation. Colorado State University., Fort Collins, 1973.
- [13] M. Frese, M. Enders-Comberg, H. Blaß and P. Glos, "Compressive strength of spruce glulam," *European Journal of Wood Products*. 70., pp. 801-809, 2012.
- [14] T. Ehrhart, R. Steiger, P. Palma and A. Frangi, "Mechanical properties of European beech glued laminated timber," *INTER Conference 51, Tallinn, Estonia, Paper 51-12-4*, 2018.
- [15] H. Blaß, "Design of timber columns," *CIB-W18 Meeting 20, Paper No. 20-2-2, Dublin, Ireland*, 1987a.
- [16] H. Blaß, "Tragfähigkeit von Druckstäben aus Brettschichtholz unter Berücksichtigung streuender Einflussgrößen. In German. Dissertation. Karlsruher Institut für Technologie," 1987b.
- [17] A. Ehret, "Mechanisches Verhalten von Buchen Brettschichtholz unter Zug- und Druckbelastung. In German. Master's Thesis. Technical University Munich," 2018.
- [18] Z-9.1-679, BS-Holz aus Buche und BS-Holz Buche-Hybridträger – Allgemeine bauaufsichtliche Zulassung, 2014.